PAPER • OPEN ACCESS

Research progress of all solid-state thin film lithium Battery

View the article online for updates and enhancements.

IOP ebooks™

Bringing you innovative digital publishing with leading voices to create your essential collection of books in STEM research.

Start exploring the collection - download the first chapter of every title for free.

Research progress of all solid-state thin film lithium Battery

XiaoPing LIANG[1], FeiHu TAN[1], Feng WEI[1], Jun DU[2,*]

[1]State Key Laboratory of Advanced Materials for Smart Sensing, General Research Institute for Non-Ferrous Metals, Beijing 101407, China

[2]General Research Institute for Non-Ferrous Metals, Beijing 100088, China

*Jun Du e-mail: dujun@grinm.com

Abstract. Compared with the traditional liquid lithium-ion battery, all solid-state lithium battery can significantly improve its safety, specific energy, specific power and cycle performance. With the development of smart society, the integration of devices has become a trend, and the corresponding energy supply system has gradually attracted attention. Among them, all solid-state thin film lithium battery is a better smart device energy unit. The deposition techniques of all solid-state thin film lithium battery are compatible with the micro-nano techniques of the micro-devices, which is conducive to the integration of the micro-devices and the micro-energy sources. This article first introduced the advantages and key issues of all solid-state thin film lithium batteries. Next, the deposition techniques of all solid-state thin film lithium batteries are introduced. Finally, the latest advances in all solid-state thin film lithium batteries are introduced, including flexible all-solid-state Thin-film lithium-ion batteries and three-dimensional structure of all-solid-state lithium-ion batteries.

1. Introduction

The development of artificial intelligence is based on self-powered smart devices. Traditional liquid lithium batteries not only have safety problems, but also do not lead to the miniaturization of the devices. All solid-state thin film lithium batteries (TFLBs) with solid electrolytes can overcome these difficulties and achieved the high energy densities through the design of structure. Therefore, TFLBs as an energy solution of smart devices has received increasing attention.

The history of TFLBs can be traced back to 1983 at Central Research Laboratory, Japan. TFLBs have become the hot topic because of lithium phosphorus oxynitride (LiPON) with high ionic conductivity developed by Bates Research Team at Oak Ridge National Laboratory, USA. In recent years, there are a series of reviews on TFLBs, including electrolytes, electrodes and key issues [1-4].The structure of TFLBs include substrate, cathode collector, cathode, solid electrolyte, anode, anode collector, and protective coating, as shown in Fig. 1.

There are series of issues of TFLBs, such as electrolyte, interface and cathode. The two key issues of TFLBs are solid electrolyte with high ionic conductivity and solid interfaces. So it is summarized that the two key issues. In order to integrate TFLBs with micro-nano devices, the deposition techniques of TFLBs is different from traditional lithium-ion batteries. At present, the deposition techniques preparing TFLBs include magnetron sputtering (MS), pulsed laser deposition (PLD), atomic layer deposition (ALD) and vacuum evaporation [5,6],etc. This paper systematically summarizes the deposition techniques of TFLBs. The structure and application of TFLBs are the latest research hotspots. The power density of TFLBs can be significantly increased by the design of three-dimensional structures (3D). The application range of TFLBs is increased by preparing the

flexible TFLBs. Therefore, this paper summarizes the latest research progress of 3D TFLBs and flexible TFLBs. This paper discusses the key issues, preparation techniques and latest developments of TFLBs, and tries to show readers the research status and focus of TFLBs.
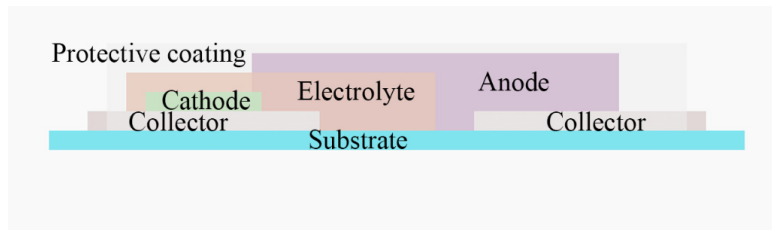

Figure 1. Structure of TFLBs

2. Key Issues of TFLBs

2.1 Electrolyte

According to a chemical composition, the solid electrolyte can be classified into the inorganic solid electrolyte, the polymer solid electrolyte, and the composite solid electrolyte. However, in order to adopt the micro-nano techniques, the inorganic solid electrolyte is generally used as the electrolyte materials of TFLBs. According to the type of crystallization, the solid electrolyte can be classified into the amorphous electrolyte and the crystalline electrolyte. The amorphous inorganic solid electrolyte can have the large change in composition, and the electrochemical properties of it also exhibit great differences. Due to the isotropic nature of the amorphous solid electrolyte, the ion diffusion channel is also isotropic. The amorphous electrolyte particles have small interfacial charge transport impedance, so that lithium ion is easy to transfer. Therefore, the main factors affecting the ion transport of the amorphous solid electrolyte are body impedance and bulk density. The crystalline inorganic solid electrolyte generally has a high lithium ion conductivity, and lithium ions can rapidly transfer through lithium vacancies or lithium gaps in the solid electrolyte lattice structure.

The solid electrolyte film is the source of high safety and excellent electrochemical performance of TFLBs, but it is also the bottleneck of TFLBs. The solid electrolyte film must meet the characteristics of high ionic conductivity, low electronic conductivity, wide electrochemical window and low electrode corrosion, etc. In order to get stable ion conductivity, it is necessary to ensure that the composition and structure of the electrolyte are controllable. Due to the presence of lithium element, the difference in element deposition rate is too large. The composition and structure of the solid electrolyte are difficult to control stably. Therefore, the solid electrolyte film can be divided into three development generations according to the control difficulty, as shown in Table 1.

Vacuum evaporation, including oxide amorphous and sulfide amorphous. Oxide solid electrolytes are chemically stable, including amorphous borate (Li_2O-B_2O_3-SiO_2), silicate (Li_2O-V_2O_5-SiO_2)[7], etc. The oxide amorphous electrolyte is composed of a network forming oxide (B_2O_3, P_2O_5, SiO_2, etc.) and a network-modified oxide (Li_2O, etc.). The network-modified oxide are prepared by adding a lithium salt, doping nitrogen and formatting the amorphous-ceramic hybrid structures[8, 9], etc. With the deepening understanding on the ion transport mechanism of oxide amorphous electrolyte, the new network forming compound is added to the original binary amorphous system to construct a ternary system. It is improved by using the "mixed network to form the bulk effect" that ion conductivity and chemical and electrochemical stability of the electrolyte system. Sulfide amorphous solid electrolytes include Li_3N, Li_2S, Li_2S-SiS_2-P_2S_5, Li_2S-GeS_2[10], etc. Although the ionic conductivity of Sulfide amorphous solid electrolytes is higher than 10^{-5} S/cm, it is deliquescent and cannot be used. The sulfide amorphous solid electrolyte is the completely substituted O in the oxide amorphous electrolyte structure. Because S is less electron-negative than O, the binding ability to lithium ions is also small. S atom radius is larger than O, and a larger ion transport channel can be formed in the network structure, which facilitates the transport of lithium ions in the structure. So the amorphous solid electrolyte has

an ionic conductivity greater than that of the oxide amorphous solid electrolyte.

Table 1. The History and Comparison of the Typical Solid Electrolyte

Categories	Period	Typical substance of solid electrolyte	Characteristics
The first	1980s	Li_3N, sulfide, amorphous borate $(Li_2O\text{-}B_2O_3\text{-}SiO_2)$、 silicate$(Li_2O\text{-}V_2O_5\text{-}SiO_2）$	easy preparation, small electrochemical window, poor stability
The second	1990-2000s	LiPON	good overall performance, low ionic conductivity
The third	2010s	Perovskite structure $[Li_{3x}La_{2/3-x}TiO_3$ (LLTO)]	high ionic conductivity, high brittleness
		Anti-perovskite structure (Li_3OCl)	high ionic conductivity, synthetic difficulty, poor environmental stability,
		NASICON structure $[Li_{1+x}Al_xTi_{2-x}(PO_4)_3$ (LATP)]	high environmental stability, high brittleness
		Garnet structure, $Li_7La_3Zr_2O_{12}$(LLZO)	high annealing temperature

The second-generation solid electrolyte is the amorphous thin film LiPON with excellent overall performance and 5.5 V electrochemical window. The ionic conductivity of LiPON is μS/cm, which is about three orders of magnitude smaller than mS/cm of the liquid electrolyte, so increasing its ionic conductivity is the key [11]. In the early years, introducing transition metal elements (Ti, Al, etc.) and non-metal elements (Si, B, etc.) to LiPON, and useing "mixed network to form bulk effects" have improved the electrical conductivity and electrochemical properties of LiPON. By adding Li_2O to the target and maintaining the N/P ratio, the activation energy of LiPON was reduced, the LiPON film without Li_2O residue had 6.4 μS/cm ionic conductivity, and it maintained the good environmental stability [12]. After the flexible TFLBs of $LiCoO_2$/LiPON/Li are repeatedly bent for 20000 times, the voltage retention rate is as high as 99.73%, and the performance after 100 cycles does not change significantly, which show the advantages of LiPON mechanics comprehensive performance. In recent years, LiPON has been fabricated into the laminated structure with the solid electrolyte having high ionic conductivity, easy large-scale preparation, and poor mechanical or chemical stability, such as LiPON/Li-PWON/LiPON [13], LiPON/LLT/LiPON [14] and LiPON/LLTO [15], in order to obtain the solid electrolyte films with better comprehensive performance.

The third generation of solid electrolyte is the crystalline film, including perovskite structure $[Li_{0.33}La_{0.56}TiO_3$ $(Li_{3x}La_{2/3-x}TiO_3$, x=0.11)], anti-perovskite structure Li_3O_X (X=Cl, Br), NASICON structure $[Li_{1+x}Al_xTi_{2-x}(PO_4)_3$ (LATP)] and garnet structure $[Li_7La_3Zr_2O_{12}$ (LLZO)]. The perovskite structure has the vacancies in the crystal structure, low activation energy (0.35eV), and ionic conductivity up to 10^{-3}S/cm. The perovskite structure needs high temperature annealing, but LLTO will exhibit heterogeneous phases such as TiO_2 after annealing, which affects its ionic conductivity. The structural stress generated by LLTO high temperature annealing increases the brittleness of the film. The TFLBs of Li/LiPON/LLTO/$LiCoO_2$/SS structure were prepared by layer deposition, and achieved 100 cycles of charge and discharge. The anti-perovskite structure has many advantages such as high ionic conductivity, low activation energy (0.2-0.3 eV), low electronic conductivity, wide electrochemical window, and high temperature resistance, receiving extensive attention. Li_3OCl has a low annealing temperature and is relatively stable to metallic lithium, providing a solution for the safety and lifetime questions in the new generation of battery systems such as sodium ion batteries [16]. The NASICON structure has good stability, is unstable to metallic lithium, has a severe grain boundary effect, and has an ionic conductivity of only 10^{-5} S/cm. However, crystalline NASICON structural films are difficult to prepare. Although NASICON structural films are unstable to lithium, they are stable in air. With the advancement of technologies such as positive and negative electrodes

and interface stability, NASICON solid electrolyte films may become indispensable materials for high performance TFLBs. The ionic conductivity of garnet structure is generally 3×10^{-4} S/cm, which has become a research hotspot in recent years due to its great comprehensive performance. However, the crystallization temperature of LLZO film exceeds 900 °C, which makes crystallization to easily lose lithium reducing the performance of battery [17].

With the deep understanding of the crystal structure, ion conduction mechanism and the further maturity of the preparation techniques, the performance of the first generation have been significantly improved; the techniques of the second generation has been established; the third generation with high ionic conductivity and practical value have become the research hotspot, providing a wide space for the development of TFLBs.

2.2 Solid Interfaces

The electrode and the electrolyte are forming space charge region due to their different lithium ion concentrations, as shown in Fig. 2. Because the electrode can conduct electrons and lithium ions, the space charge area disappears. Due to the only ions conductor solid electrolyte, there is a lithium-deficient space charge region.

The insufficient contact area between electrode and electrolyte results in the large interface impedance. The oxidation or reduction reaction of the solid electrolyte occurs to form the solid interface, because of the bad stability of it. When the battery is charging and discharging, the solid electrolyte is forming by inter-diffusion of lithium ions. Due to the change of the electrode in volume at the solid interface, the excessive stress at the solid interface cause poor contact or the increasing internal resistance, spatial separation. Therefore, the key to solving the issue of the solid interface is to suppress the space charge area, increase the contact area, and reduce the interfacial stress.
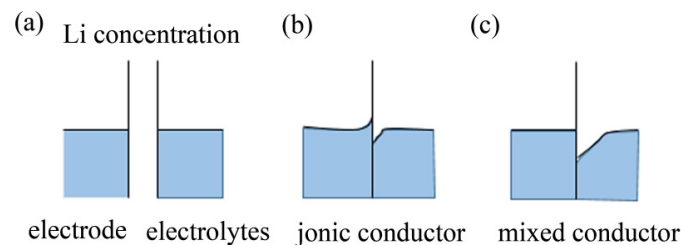

Figure 2. Li concentration change at solid interface

There are several reports about to modify the solid interface of TFLBs. The introduction of interlayer can generally achieve the modification of the solid interfaces in TFLBs. NbO_2 interlayer is introduced between $LiCoO_2$ cathode and the electrolyte to reduce the interfacial stress [18]. Al_2O_3 interlayer is introduced between $LiCoO_2$ and LiPON, decreasing the interfacial resistance [45]. $Li_4Ti_5O_{12}$ or $LiNbO_3$ [20, 21] coats $LiCoO_2$ by spraying techniques to suppress the formation of the space charge layer. The Si interlayer with the thickness of 20 nm is deposited on lithium metal to inhibits the reduction of the electrolyte [22].Thermal annealing can modify the solid interfaces, which significantly reduces charge transfer resistance. The solid interfaces can be modified by increasing interfacial contact area through depositing the oxide interlayer.

3. Deposition Techniques

The deposition techniques of TFLBs can be divided into two categories, physical vapor deposition (PVD) and Chemical Vapor Deposition (CVD). PVD is a technique in which a material source is vaporized into a gaseous atom, a molecule or a partially ionized ion under a vacuum condition, and a film having a specific function is deposited on the surface of the substrate by a low-pressure gas (or plasma). The main methods of PVD include vacuum evaporation, sputtering and ion plating, etc.

PVD can deposit not only metal films, alloy films, but also compounds, ceramics, semiconductors, polymer films, etc. CVD is mainly a technique, forming a thin film by chemical reaction on the surface of a substrate using one or several gas phase compounds or simple substances. CVD can be used to deposit various single crystal, polycrystalline or glassy inorganic thin film materials. The comparison of different deposition technique is shown in Table 2.

3.1 MS

MS is a kind of PVD, preparing a plurality of materials such as metal, semiconductor, insulator. MS has the advantages of easy control, large coating area, and strong adhesion of films.

MS can be used to deposit the solid electrolyte thin films. An amorphous electrolyte film with 1.22×10^{-6} S/cm ionic conductivity was prepared by using Li_2O-B_2O_3-P_2O_5 as a target [23]. Using amorphous oxide electrolyte target, Li-BPON film has an ionic conductivity of up to 3.5×10^{-6} S/cm and an activation energy of only 0.53 eV prepared by reactive sputtering under N_2 atmosphere [14]. The ion conductivity of Li_6GeS_5 electrolyte film prepared by MS is up to 1.7×10^{-3} S/cm [24]. An amorphous thin film LiPON with the ion conductivity of 3.3×10^{-6} S/cm was deposited by reactive sputtering principle [25,26]. The N content has a great influence on the performance of LiPON film [27], and other influencing factors including pressure, target-substrate distance, and target density are the main factors [28,29]. The ionic conductivity of the perovskite solid electrolyte prepared by magnetron sputtering is 5.2×10^{-5} S/cm [30]. The ionic conductivity of the anti-perovskite electrolyte prepared by magnetron sputtering is 8.9×10^{-6} S/cm [31]. Amorphous Li-Si-Ti-PON film prepared by MS under N_2 gas, with NASICON structure $LiTi_2(PO_4)_3$ as the target, has the ion conductivity of 9.2×10^{-6} S/cm [32]. A crystalline NASICON structured solid deposited on the ITO amorphous surface by increasing the substrate temperature to 400 °C in 65% Ar+35%O_2 atmosphere , with $Li_{1.3}Al_{0.3}Ti_{1.7}(PO_4)_3$ as the target, has an ionic conductivity of 2.46×10^{-5} S/cm [33]. Using sintered ceramics as a target, in a pure N_2 atmosphere, the ionic conductivity of Li-Al-Ti-PON prepared by MS was 1.22×10^{-5} S/cm [34]. Magnetron sputtering causes loss of lithium and affects the performance of the electrolyte. The ionic conductivity of the amorphous structure LLTO thin film by MS is 9.4×10^{-7} S/cm [35]. The LLTO film by annealing can get the internal structure of the film to reach or approach equilibrium, further eliminating defects [36]. The general MS depositing LLTO films requires consideration of substrate temperature, substrate orientation and annealing [25], etc. The crystallization temperature of the garnet structure is too high, so the preparation of the amorphous LLZO film is relatively not easy. The Li-La-Ti-Zr-O film prepared by co-sputtering using LLTO and LLZO targets has an ionic conductivity of 2.83×10^{-6} S/cm [37]. The Li-La-Zr-O amorphous film was prepared on SiO_2-Si sheets by RF magnetron sputtering with an ionic conductivity of 4×10^{-7} S/cm [38]. Li ion conductivity of LLZO was determined to be 1.2×10^{-4} S/cm at room temperature and the activation energy was determined to be 0.47 eV [39].

MS can be used to deposit the cathode electrode thin film. $LiCoO_2$ films can be deposited by MS, and rapid annealing can reduce film cracking. The $LiCoO_2$ film prepared by the improved MS has a specific capacity of 110 mA•h/g. $LiCoO_2$ film having (101) oriented crystal plane facilitates the transport of lithium ions [40, 41]. The thickness of the $LiCoO_2$ film is related to battery attenuation and discharge capacity. By preparing the $LiCoO_2$/Ag/$LiCoO_2$/Ag/$LiCoO_2$ structure film with (101) and (104) crystal planes, the rate characteristics of the battery can be improved [42]. The FeS_2 film with a thickness of 365 nm was prepared by MS, and its volume specific capacity was 5 times that of $LiCoO_2$ film [43]. The crystalline V_2O_5 film can also be prepared by MS, and its thickness affects the battery cyclic performance [44]. Li-Co-Ni-Mn-O film can be deposited by MS, of which (110) surface-oriented film amorphous has the best rate performance [45]. The spinel-type cathode electrode can be prepared by MS. The spinel structure of $LiMn_2O_4$ film as a cathode electrode has good cycle performance [46]. MS can prepare the lithium manganese-based cathode electrode film with a high specific capacity. The key factor affecting the performance of the cathode film is the stoichiometric ratio of the target.

MS can be used to prepare component gradient and non-gradient SiCu film anodes. The Cu-rich region in the gradient film helps to reduce the accumulation of stress inside the film, thus preventing

the cracking of the film in the cycle. $Si_{1-x}C_x$ films with different carbon contents can be deposited by MS [47]. The SnOx/C composite anode film was prepared by MS, and the carbon played the role of electron conductance in the film and relieved the effect of volume expansion [48]. $Li_4Ti_5O_{12}$ and TiO_2 anode films were also prepared by magnetron sputtering [49-51].

MS can prepare different thin films of TFLBs, so TFLBs can be prepared by MS. However, problems such as lithium element loss and film uniformity caused by MS still require further exploration.

Table 2. The Comparison of different deposotion techniques

Categories	Deposotion Techniques	Characteristics	Application
PVD	MS	fast deposition rate, loss of lithium, big composition segregation	cathode, solid electrolyte, anode, TFLBs
	PLD	small composition segregation, low deposition temperature, poor film uniformity	cathode, solid electrolyte, anode
	Vacuum Evaporation	simple equipment, fast deposition rate, poor adhesion and poor repeatability	cathode, solid electrolyte, anode
	Ion-beam Sputtering	slow deposition rate, good film quality, poor adhesion	solid electrolyte
CVD	PECVD	low deposition temperature, good film quality, good adhesion	cathode
	LCVD	fast deposition rate, good adhesion	cathode
	LPCVD	good film uniformity	solid electrolyte , anode
	MOCVD	low deposition temperature, slow deposition rate, poor film quality	solid electrolyte
	ALD	slow deposition rate, good film uniformity and quality	cathode, solid electrolyte, anode

3.2 PLD
PLD belongs PVD technique, which is a technique of bombarding an object with a laser and then depositing the bombarded material on substrates to obtain the thin film. The film prepared by PLD technique has the advantages of small composition segregation and low deposition temperature.

The solid electrolyte can be deposited by PLD. The ionic conductivity of Li_2S-GeS_2 solid electrolyte prepared by PLD is 1.8×10^{-4} S/cm [23]. The ionic conductivity of LiPON by PLD can reach 1.6×10^{-6} S/cm, which can be realized to deposit on flexible substrates, such as carbon tube and mica [52]. The ionic conductivity of the perovskite electrolyte by PLD was 6.7×10^{-4} S/cm [53]. The preparation of LLTO by PLD requires to consider the influence of substrate temperature and substrate orientation on the properties [54]. The solid electrolyte ionic conductivity of the anti-perovskite structure by PLD is 0.9×10^{-5} S/cm [55]. The electrolyte ion conductivity of the NASICON structure is 2.46×10^{-5} S/cm [28]. The ionic conductivity of the garnet structure is 1.0×10^{-5} S/cm [56].

The cathode V_2O_5 film, $LiCoO_2$ film, spinel $LiFePO_4$ film and $LiCoO_2$ film can all be prepared by PLD. The $LiMn_2O_4$ film with a preferred orientation of (111) crystal plane and good crystallinity was prepared by PLD at the substrate temperature of 700 °C [57]. The $LiMnPO_4$ cathode thin film has lower electron conductivity and ionic conductivity at a substrate temperature of 600 °C [58]. The $LiNi_{1-y}M_yO_2$ (M=Co, Al) film doped with Co and Al was prepared by PLD technique. Attention should be paid to

the substrate temperature and the oxygen pressure of the cavity during deposition [59]. $LiNi_{0.5}Mn_{1.5}O_4$ and spinel $LiCoMnO_4$ films can also be deposited by PLD technique [60,61].

The Mg_2Si anode film was prepared by PLD technique. The specific capacity of this anode film reached 2000 mA•h/g in the range of 0.1~1 V, and there was no significant attenuation after 100 cycles [62]. The SiCu anode film can be prepared by PLD [63]. The SnO film by PLD has poor cycle performance [64]. $Li_4Ti_5O_{12}$ and TiO_2 anode films can be deposited by PLD [65,66]. Novel anodes, such as $TiNb_2O_7$ thin film or NiO–NiSe nanocomposite, can also be prepared by PLD [67, 68].

PLD can deposit cathode, electrolyte and anode films. The substrate temperature and the deposited oxygen pressure are two deposition parameters that are of particular interest when preparing the film.

3.3 Vacuum Evaporation

Vacuum evaporation is a kind of PVD. The material evaporates under certain heating conditions and flies to the surface of substrate to form a thin film. Evaporation is an early and widely used vapor deposition technique, which has the advantages of simple film technique, high film purity and high compactness. The evaporation source of vacuum evaporation includes the electric resistance, an electron beam, the high frequency method and the laser, etc.

LiPON and LLTO electrolyte films can be prepared by vacuum evaporation [15]. The cathode V_2O_5 film and the metal lithium anode electrode can be prepared by vacuum evaporation technique [69].

3.4 Ion-beam Sputtering

Ion-beam sputtering, belonging to PVD, uses the ion source to generate a certain amount of energy to bombard the target under high vacuum, causing it to be sputtered out and deposited on the substrate to form a film. LiPON films can be prepared by ion-beam sputtering with an ionic conductivity of 6.0×10^{-7} S/cm [70].

3.5 CVD

CVD can deposit thin film of TFLBs. Low-pressure chemical vapor deposition (LPCVD) utilizes the characteristics of increased gas diffusion coefficient at low pressure to accelerate the transport rate of gaseous reactants and by-products, increase the reaction rate of forming thin films, and prepare $LiCoO_2$ cathode electrode film [71]. Plasma-enhanced chemical vapor deposition (PECVD) uses a kinetic energy of electrons in a plasma to excite the chemical vapor phase reaction, preparing the spinel $LiMn_2O_4$ cathode electrode film [72]. Laser chemical vapor deposition (LCVD) is a thin film deposition technique in which a laser is used as the heating heat source to induce a gas phase reaction. LCVD can be deposited the anode electrode film TiO_2 and an electrolyte film Garnet-type $Li_7La_3Zr_2O_{12}$ [73,74]. Metal-organic chemical vapor deposition (MOCVD) is to transfer the metal alkyl compound and other components into the reaction chamber, and then the metal organic compound decomposes to deposit the metal or compound film. The LiPON electrolyte film by MOCVD has an ionic conductivity of 2.96×10^{-7} S/cm [75].

3.6 ALD

ALD is a technique in which the film can be deposited by layer by layer monoatomic film. ALD is similar to ordinary chemical deposition. However, in the atomic layer deposition process, the chemical reaction of the new atomic film is directly related to the previous layer, in such a way that only one layer of atoms is deposited per reaction.

ALD technique can be used to prepare 3D TFLBs. LiPON with an ionic conductivity of 6.6×10^{-7} S/cm can be deposited by ALD [76]. The ionic conductivity of the perovskite structure solid electrolyte by ALD is 2×10^{-8} S/cm [77]. The cathode V_2O_5 and $LiCoO_2$ films can be depositde by ALD [78,79]. ALD can deposit TiO_2 and Co_3O_4 anode electrode film [80,81], and can also be used to prepare nanostructured anode electrode, such as Core-shell $Si@ TiO_2$ nanosphere anode.
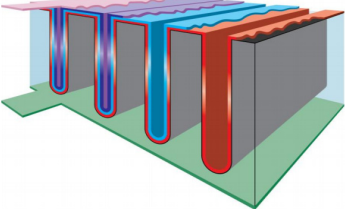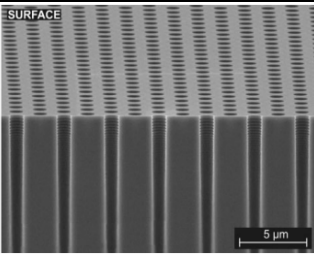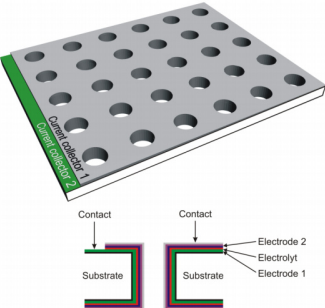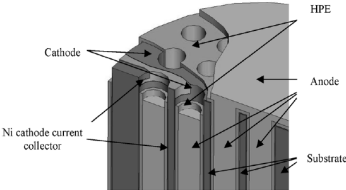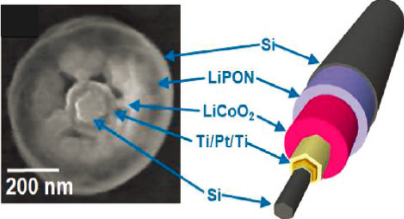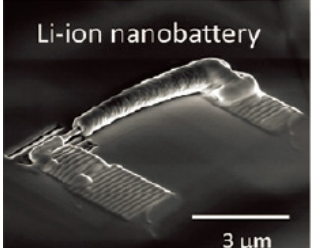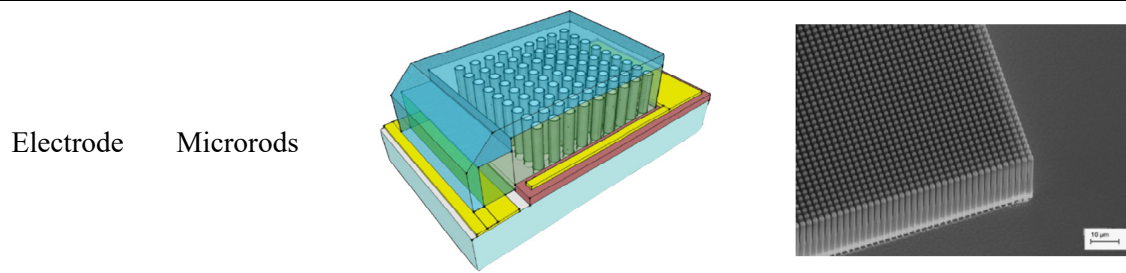
4. Latest Advances in TFLBs

4.1 3D TFLBs

3D TFLBs can reduce the volume occupied by inactive materials as substrate and packaging, so it increases the volumetric energy density of batteries. 3D TFLBs also enlarge the internal surface area between cathode, electrolyte and anode, meaning that batteries have higher current. 3D TFLBs should have relatively high current and power density. The schematics of 3D TFLBs are listed in Table 3.

3D TFLBs can be achieved by changing the substrate structure. Forming microholes in the substrate, these microholes provide good support for insulation between the cells. Thin films sequentially are deposited in the holes to prepare batteries[82], and the battery structure can be integrated with solar cells. Microchannels are formed in the substrate[83,84], which have a typical radius between 15 and 50 µm. Stack comprising of cathode current collector, cathode, the solid electrolyte, anode, anode current collector, these thin films are deposited by PVD or CVD. The substrate is prepared into the special structure, of which the battery is depositde on surface [85]. The fibrous TFLBs is prepared by depositing functional layers on the surface of the nano silicon wire, so that the battery is expected to be wearable device. Because the diameter of the battery is only a few hundred nanometers, it is possible to directly observe the changes in microstructure and surface topography of the battery during charge and discharge.

3D TFLBs can also be implemented by the three-dimensional structure of the electrode. Silicon microrods as anode were prepared by deep reactive ion etching in-situ directly on the silicon wafer, and then LiPON and LiFePO$_4$ were deposited separately to form the battery [86]. Microrods can also be constructed by photolithography and etching [87]. Both cathode electrode and anode electrode can be fabricated into microrods structure to realize the preparation of 3D TFLBs.

Table 3. The schematics of 3D TFLBs

Change	Structure	Schematic	Instance
	Microholes		
Substrate	Microchannels		
	Fibrous		

Electrode   Microrods

4.2 Flexible TFLBs

Flexible TFLBs can be applied to the wearable devices, and the flexibility of its structure can broaden the breadth and depth of application of TFLBs. Flexible TFLBs with 10 C discharge were prepared by continuous deposition and rapid annealing using flexible mica as substrate [40]. However, the metallic lithium anode has poor environmental stability. 300 nm thick Ti film and 300 nm LiPO film are used as a protective layer, so that 3 μm thick metal lithium anode electrode is stably present in the air for 1 h[88]. Research on Flexible TFLBs has received much attention. Flexible TFLBs with $LiCoO_2$/LiPON/Li structure have been prepared. After repeated bending for 20,000 times, the voltage retention rate is as high as 99.73%. The Flexible TFLBs are stripped from the mica substrate, wrapped in the PDMS. OLED is integrated with it to form a flexible device integrating the energy storage and the display screen [89], as shown in Figure 3.

Figure 3. Schematic diagram and picture of flexible LED system integrated with Flexible TFLBs[89]

5. Summary

The research of solid electrolyte with good stability and high ionic conductivity and the solid-state interfaces are still key issues that constrain the performance of TFLBs. The deposition techniques of TFLBs need to consider cost and compatibility with micro-nano devices. 3D TFLBs and Flexible TFLBs not only increase the power density of TFLBs, but also extend the application of TFLBs. The development of TFLBs requires attention to three aspects of materials, techniques and structures.

Acknowledgement

References

[1]   Quartarone, E., & Mustarelli, P. (2011) Electrolytes for solid-state lithium rechargeable batteries: recent advances and perspectives. Chemical Society Reviews, 40(5), 2525-2540.

[2] Zhou, Y. N., Xue, M. Z., & Fu, Z. W. (2013) Nanostructured thin film electrodes for lithium storage and all-solid-state thin-film lithium batteries. Journal of Power Sources, 234, 310-332.

[3] Oudenhoven, J. F., Baggetto, L., & Notten, P. H. (2011) All-solid-state lithium-ion microbatteries: a review of various three‐dimensional concepts. Advanced Energy Materials, 1(1), 10-33.

[4] Roberts, M., Johns, P., Owen, J., Brandell, D., Edstrom, K., El Enany, G., ... & Mazor, H. (2011) 3D lithium ion batteries—from fundamentals to fabrication. Journal of Materials Chemistry, 21(27), 9876-9890.

[5] Wartena, R., Curtright, A. E., Arnold, C. B., Piqué, A., & Swider-Lyons, K. E. (2004) Li-ion microbatteries generated by a laser direct-write method. Journal of Power Sources, 126(1-2), 193-202.

[6] Bates, J. B., Dudney, N. J., Neudecker, B., Ueda, A., & Evans, C. D. (2000) Thin-film lithium and lithium-ion batteries. Solid state ionics, 135(1-4), 33-45.

[7] Muñoz, F., Montagne, L., Pascual, L., & Durán, A. (2009) Composition and structure dependence of the properties of lithium borophosphate glasses showing boron anomaly. Journal of Non-Crystalline Solids, 355(52-54), 2571-2577.

[8] Karan, N. K., Natesan, B., & Katiyar, R. S. (2006) Structural and lithium ion transport studies in borophosphate glasses. Solid State Ionics, 177(17-18), 1429-1436.

[9] Wu, F., Zheng, Y., Li, L., Tan, G., Chen, R., & Chen, S. (2013) Novel Micronano Thin Film Based on Li–B–P–O Target Incorporating Nitrogen as Electrolyte: How Does Local Structure Influence Chemical and Electrochemical Performances?. The Journal of Physical Chemistry C, 117(38), 19280-19287.

[10] ZHANG, S., WANG, S., LING, S., Gao, J., Wu, J., Xiao, R., ... & Chen, L. (2014) Fundamental scientific aspects of lithium ion batteries (X)--All-solid-state lithium-ion batteries. Energy Storage Science and Technology, 3(4), 376-394.

[11] Put, B., Vereecken, P. M., Meersschaut, J., Sepúlveda, A., & Stesmans, A. (2016) Electrical characterization of ultrathin RF-sputtered LiPON layers for nanoscale batteries. ACS applied materials & interfaces, 8(11), 7060-7069.

[12] Suzuki, N., Shirai, S., Takahashi, N., Inaba, T., & Shiga, T. (2011) A lithium phosphorous oxynitride (LiPON) film sputtered from unsintered Li3PO4 powder target. Solid State Ionics, 191(1), 49-54.

[13] Jee, S. H., Lee, M. J., Ahn, H. S., Kim, D. J., Choi, J. W., Yoon, S. J., ... & Yoon, Y. S. (2010) Characteristics of a new type of solid-state electrolyte with a LiPON interlayer for Li-ion thin film batteries. Solid State Ionics, 181(19-20), 902-906.

[14] min Lee, J., ho Kim, S., Tak, Y., & Yoon, Y. S. (2006) Study on the LLT solid electrolyte thin film with LiPON interlayer intervening between LLT and electrodes. Journal of power sources, 163(1), 173-179.

[15] Li, C. L., Zhang, B., & Fu, Z. W. (2006) Physical and electrochemical characterization of amorphous lithium lanthanum titanate solid electrolyte thin-film fabricated by e-beam evaporation. Thin solid films, 515(4), 1886-1892.

[16] Mouta, R., Melo, M. A. B., Diniz, E. M., & Paschoal, C. W. A. (2014) Concentration of Charge Carriers, Migration, and Stability in Li3OCl Solid Electrolytes. Chemistry of Materials, 26(24), 7137-7144.

[17] Teng, S., Tan, J., & Tiwari, A. (2014) Recent developments in garnet based solid state electrolytes for thin film batteries. Current Opinion in Solid State and Materials Science, 18(1), 29-38.

[18] Okumura, T., Nakatsutsumi, T., Ina, T., Orikasa, Y., Arai, H., Fukutsuka, T., ... & Ogumi, Z. (2011) Depth-resolved X-ray absorption spectroscopic study on nanoscale observation of the electrode–solid electrolyte interface for all solid state lithium ion batteries. Journal of Materials Chemistry, 21(27), 10051-10060.

[19] Jeong, E., Hong, C., Tak, Y., Nam, S. C., & Cho, S. (2006) Investigation of interfacial resistance between LiCoO2 cathode and LiPON electrolyte in the thin film battery. Journal of power sources, 159(1), 223-226.

[20] Ohta, N., Takada, K., Zhang, L., Ma, R., Osada, M., & Sasaki, T. (2006) Enhancement of the high‐rate capability of solid‐state lithium batteries by nanoscale interfacial modification. Advanced Materials, 18(17), 2226-2229.

[21] Ohta, N., Takada, K., Sakaguchi, I., Zhang, L., Ma, R., Fukuda, K., ... & Sasaki, T. (2007) LiNbO3-coated LiCoO2 as cathode material for all solid-state lithium secondary batteries. Electrochemistry communications, 9(7), 1486-1490.

[22] Ogawa, M., Kanda, R., Yoshida, K., Uemura, T., & Harada, K. (2012) High-capacity thin film lithium batteries with sulfide solid electrolytes. Journal of Power Sources, 205, 487-490.

[23] Yoon, Y., Park, C., Kim, J., & Shin, D. (2013) The mixed former effect in lithium borophosphate oxynitride thin film electrolytes for all-solid-state micro-batteries. Electrochimica Acta, 111, 144-151.

[24] Seo, I., & Martin, S. W. (2011) Fast lithium ion conducting solid state thin-film electrolytes based on lithium thio-germanate materials. Acta Materialia, 59(4), 1839-1846.

[25] Bates, J. B., Gruzalski, G. R., Dudney, N. J., Luck, C. F., Yu, X. H., & Jones, S. D. (1993) Rechargeable thin-film lithium microbatteries. Solid state technology, 36(7), 59-64.

[26] Bates, J. B., Dudney, N. J., Gruzalski, G. R., Zuhr, R. A., Choudhury, A., Luck, C. F., & Robertson, J. D. (1992) Electrical properties of amorphous lithium electrolyte thin films. Solid state ionics, 53, 647-654.

[27] Su, Y., Falgenhauer, J., Polity, A., Leichtweiß, T., Kronenberger, A., Obel, J., ... & Meyer, B. K. (2015) LiPON thin films with high nitrogen content for application in lithium batteries and electrochromic devices prepared by RF magnetron sputtering. Solid State Ionics, 282, 63-69.

[28] Hamon, Y., Douard, A., Sabary, F., Marcel, C., Vinatier, P., Pecquenard, B., & Levasseur, A. (2006) Influence of sputtering conditions on ionic conductivity of LiPON thin films. Solid State Ionics, 177(3-4), 257-261.

[29] Fleutot, B., Pecquenard, B., Martinez, H., Letellier, M., & Levasseur, A. (2011) Investigation of the local structure of LiPON thin films to better understand the role of nitrogen on their performance. Solid State Ionics, 186(1), 29-36.

[30] Xiong, Y., Tao, H., Zhao, J., Cheng, H., & Zhao, X. (2011) Effects of annealing temperature on structure and opt-electric properties of ion-conducting LLTO thin films prepared by RF magnetron sputtering. Journal of Alloys and Compounds, 509(5), 1910-1914.

[31] Lü, X., Howard, J. W., Chen, A., Zhu, J., Li, S., Wu, G., ... & Jia, Q. (2016) Antiperovskite Li3OCl Superionic Conductor Films for Solid‐State Li‐Ion Batteries. Advanced Science, 3(3), 1500359.

[32] Wu, F., Liu, Y., Chen, R., Chen, S., & Wang, G. (2009) Preparation and performance of novel Li–Ti–Si–P–O–N thin-film electrolyte for thin-film lithium batteries. Journal of Power Sources, 189(1), 467-470.

[33] Chen, H., Tao, H., Zhao, X., & Wu, Q. (2011) Fabrication and ionic conductivity of amorphous Li–Al–Ti–P–O thin film. Journal of Non-Crystalline Solids, 357(16-17), 3267-3271.

[34] Tan, G., Wu, F., Li, L., Liu, Y., & Chen, R. (2012) Magnetron sputtering preparation of nitrogen-incorporated lithium–aluminum–titanium phosphate based thin film electrolytes for all-solid-state lithium ion batteries. The Journal of Physical Chemistry C, 116(5), 3817-3826.

[35] Chen, R., Liang, W., Zhang, H., Wu, F., & Li, L. (2012) Preparation and performance of novel LLTO thin film electrolytes for thin film lithium batteries. Chinese Science Bulletin, 57(32), 4199-4204.

[36] Kim, S., Hirayama, M., Cho, W., Kim, K., Kobayashi, T., Kaneko, R., ... & Kanno, R. (2014) Low temperature synthesis and ionic conductivity of the epitaxial Li 0.17 La 0.61 TiO 3 film electrolyte. CrystEngComm, 16(6), 1044-1049.

[37] Nong, J., Xu, H., Yu, Z., Zhu, G., & Yu, A. (2015) Properties and preparation of Li–La–Ti–Zr–O thin film electrolyte. Materials Letters, 154, 167-169.

[38] Kalita, D. J., Lee, S. H., Lee, K. S., Ko, D. H., & Yoon, Y. S. (2012) Ionic conductivity properties of amorphous Li–La–Zr–O solid electrolyte for thin film batteries. Solid State Ionics, 229, 14-19.

[39] Lobe, S., Dellen, C., Finsterbusch, M., Gehrke, H. G., Sebold, D., Tsai, C. L., ... & Guillon, O. (2016) Radio frequency magnetron sputtering of Li7La3Zr2O12 thin films for solid-state batteries. Journal of power sources, 307, 684-689.

[40] Song, S. W., Choi, H., Park, H. Y., Park, G. B., Lee, K. C., & Lee, H. J. (2010) High rate-induced structural changes in thin-film lithium batteries on flexible substrate. Journal of Power Sources, 195(24), 8275-8279.

[41] Yoon, Y., Park, C., Kim, J., & Shin, D. (2013) Lattice orientation control of lithium cobalt oxide cathode film for all-solid-state thin film batteries. Journal of Power Sources, 226, 186-190.

[42] Wook, J. S., & Lee, S. M. (2007) LiCoO2∕ Ag Multilayer Film Cathodes for Thin-Film Rechargeable Lithium Batteries. Journal of the Electrochemical Society, 154(1), A22-A25.

[43] Pelé, V., Flamary, F., Bourgeois, L., Pecquenard, B., & Le Cras, F. (2015) Perfect reversibility of the lithium insertion in FeS2: The combined effects of all-solid-state and thin film cell configurations. Electrochemistry Communications, 51, 81-84.

[44] Jeon, E. J., Shin, Y. W., Nam, S. C., Cho, W. I., & Yoon, Y. S. (2001) Characterization of All-Solid-State Thin-Film Batteries with V 2 O 5 Thin-Film Cathodes Using Ex Situ and In Situ Processes. Journal of The Electrochemical Society, 148(4), A318-A322.

[45] Tan, G., Wu, F., Lu, J., Chen, R., Li, L., & Amine, K. (2014) Controllable crystalline preferred orientation in Li–Co–Ni–Mn oxide cathode thin films for all-solid-state lithium batteries. Nanoscale, 6(18), 10611-10622.

[46] Lee, K. L., Jung, J. Y., Lee, S. W., Moon, H. S., & Park, J. W. (2004) Electrochemical characteristics and cycle performance of LiMn2O4/a-Si microbattery. Journal of power sources, 130(1-2), 241-246.

[47] Jiménez, A. R., Winter, M., & Placke, T. (2016). Structural Influence of Magnetron-Sputtered Silicon-Carbon Thin Films on the Anode Performance in Lithium-Ion Batteries. In: The Electrochemical Society. Honolulu. No. 2, pp. 162-162.

[48] Park, S., Lee, K. S., & Yoon, Y. S. (2016) Designing SnOx/C films via co-sputtering as anodes for all-solid-state batteries. Surface and Coatings Technology, 294, 139-144.

[49] Wunde, F., Berkemeier, F., & Schmitz, G. (2012) Lithium diffusion in sputter-deposited Li4Ti5O12 thin films. Journal of Power Sources, 215, 109-115.

[50] Zhu, J., Zeng, K., & Lu, L. (2012) Cycling effects on interfacial reliability of TiO 2 anode film in thin film lithium-ion microbatteries. Journal of Solid State Electrochemistry, 16(5), 1877-1881.

[51] Gockeln, M., Glenneberg, J., Busse, M., Pokhrel, S., Mädler, L., & Kun, R. (2018) Flame aerosol deposited Li4Ti5O12 layers for flexible, thin film all-solid-state Li-ion batteries. Nano Energy, 49, 564-573.

[52] Zhao, S. L., Wen, J. B., Zhu, Y. M., & QIN, Q. Z. (2008) Fabrication and electrochemical properties of all solid state 0.3 Ag-V~ 2O~ 5| LiPON| Li thin film battery. Journal of Functional Materials, 39(1), 91.

[53] Wei, J., Ogawa, D., Fukumura, T., Hirose, Y., & Hasegawa, T. (2015) Epitaxial strain-controlled ionic conductivity in Li-ion solid electrolyte Li0. 33La0. 56TiO3 thin films. Crystal Growth & Design, 15(5), 2187-2191.

[54] Kim, S., Hirayama, M., Suzuki, K., & Kanno, R. (2014) Hetero-epitaxial growth of Li0. 17La0. 61TiO3 solid electrolyte on LiMn2O4 electrode for all solid-state batteries. Solid State Ionics, 262, 578-581.

[55] Lü, X., Wu, G., Howard, J. W., Chen, A., Zhao, Y., Daemen, L. L., & Jia, Q. (2014) Li-rich anti-perovskite Li 3 OCl films with enhanced ionic conductivity. Chemical Communications, 50(78), 11520-11522.

[56] Kim, S., Hirayama, M., Taminato, S., & Kanno, R. (2013) Epitaxial growth and lithium ion conductivity of lithium-oxide garnet for an all solid-state battery electrolyte. Dalton Transactions, 42(36), 13112-13117.

[57] Otsuji, H., Kawahara, K., Ikegami, T., & Ebihara, K. (2006) LiMn2O4 thin films prepared by pulsed laser deposition for rechargeable batteries. Thin Solid Films, 506, 120-122.

[58] Fujimoto, D., Kuwata, N., Matsuda, Y., Kawamura, J., & Kang, F. (2015) Fabrication of solid-state thin-film batteries using LiMnPO4 thin films deposited by pulsed laser deposition. Thin Solid Films, 579, 81-88.

[59] Ramana, C. V., Zaghib, K., & Julien, C. M. (2006) Synthesis, structural and electrochemical properties of pulsed laser deposited Li (Ni, Co) O2 films. Journal of power sources, 159(2), 1310-1315.

[60] Wang, Y., Yang, G., Yang, Z., Zhang, L., Fu, M., Long, H., ... & Lu, P. (2013) High power and capacity of LiNi0. 5Mn1. 5O4 thin films cathodes prepared by pulsed laser deposition. Electrochimica Acta, 102, 416-422.

[61] Kuwata, N., Kudo, S., Matsuda, Y., & Kawamura, J. (2014) Fabrication of thin-film lithium batteries with 5-V-class LiCoMnO4 cathodes. Solid State Ionics, 262, 165-169.

[62] Song, S. W., Striebel, K. A., Reade, R. P., Roberts, G. A., & Cairns, E. J. (2003) Electrochemical studies of nanoncrystalline Mg2Si thin film electrodes prepared by pulsed laser deposition. Journal of The Electrochemical Society, 150(1), A121-A127.

[63] Hang, B. T., Ohnishi, T., Osada, M., Xu, X., Takada, K., & Sasaki, T. (2010) Lithium silicon sulfide as an anode material in all-solid-state lithium batteries. Journal of Power Sources, 195(10), 3323-3327.

[64] Kuwata, N., Kawamura, J., Toribami, K., Hattori, T., & Sata, N. (2004) Thin-film lithium-ion battery with amorphous solid electrolyte fabricated by pulsed laser deposition. Electrochemistry Communications, 6(4), 417-421.

[65] Deng, J., Lu, Z., Belharouak, I., Amine, K., & Chung, C. Y. (2009) Preparation and electrochemical properties of Li4Ti5O12 thin film electrodes by pulsed laser deposition. Journal of Power Sources, 193(2), 816-821.

[66] Yamamoto, S., Sumita, T., Miyashita, A., & Naramoto, H. (2001) Preparation of epitaxial TiO2 films by pulsed laser deposition technique. Thin Solid Films, 401(1-2), 88-93.

[67] Daramalla, V., Penki, T. R., Munichandraiah, N., & Krupanidhi, S. B. (2016) Fabrication of TiNb2O7 thin film electrodes for Li-ion micro-batteries by pulsed laser deposition. Materials Science and Engineering: B, 213, 90-97.

[68] Yang, Y., Liu, J., Dai, H. Q., Cui, Y., Liu, J., Liu, X., & Fu, Z. W. (2016) Pulsed laser deposited NiO–NiSe nanocomposite as a new anode material for lithium storage. Journal of Alloys and Compounds, 661, 190-195.

[69] Lee, S. H., Liu, P., Tracy, C. E., & Benson, D. K. (1999) All‐Solid‐State Rocking Chair Lithium Battery on a Flexible Al Substrate. Electrochemical and solid-state letters, 2(9), 425-427.

[70] Nowak, S., Berkemeier, F., & Schmitz, G. (2015) Ultra-thin LiPON films–Fundamental properties and application in solid state thin film model batteries. Journal of Power Sources, 275, 144-150.

[71] Oudenhoven, J. F. M., Van Dongen, T., Niessen, R. A. H., De Croon, M. H. J. M., & Notten, P. H. L. (2009) Low-pressure chemical vapor deposition of LiCoO2 thin films: a systematic

investigation of the deposition parameters. Journal of The Electrochemical Society, 156(5), D169-D174.

[72] Liu, P., Zhang, J. G., Turner, J. A., Tracy, C. E., & Benson, D. K. (1999) Lithium‐Manganese‐Oxide Thin‐Film Cathodes Prepared by Plasma‐Enhanced Chemical Vapor Deposition. Journal of the Electrochemical Society, 146(6), 2001-2005.

[73] Guo, D., Ito, A., Goto, T., Tu, R., Wang, C., Shen, Q., & Zhang, L. (2013) Preparation of rutile TiO 2 thin films by laser chemical vapor deposition method. Journal of Advanced Ceramics, 2(2), 162-166.

[74] Loho, C., Djenadic, R., Bruns, M., Clemens, O., & Hahn, H. (2017) Garnet-type Li7La3Zr2O12 solid electrolyte thin films grown by CO2-laser assisted CVD for all-solid-state batteries. Journal of The Electrochemical Society, 164(1), A6131-A6139.

[75] Kim, H. T., Mun, T., Park, C., Jin, S. W., & Park, H. Y. (2013) Characteristics of lithium phosphorous oxynitride thin films deposited by metal-organic chemical vapor deposition technique. Journal of Power Sources, 244, 641-645.

[76] Kozen, A. C., Pearse, A. J., Lin, C. F., Noked, M., & Rubloff, G. W. (2015) Atomic layer deposition of the solid electrolyte LiPON. Chemistry of Materials, 27(15), 5324-5331.

[77] Liu, J., Banis, M. N., Li, X., Lushington, A., Cai, M., Li, R., ... & Sun, X. (2013) Atomic layer deposition of lithium tantalate solid-state electrolytes. The Journal of Physical Chemistry C, 117(39), 20260-20267.

[78] Chen, X., Pomerantseva, E., Banerjee, P., Gregorczyk, K., Ghodssi, R., & Rubloff, G. (2012) Ozone-based atomic layer deposition of crystalline V2O5 films for high performance electrochemical energy storage. Chemistry of Materials, 24(7), 1255-1261.

[79] Xie, M., Sun, X., Sun, H., Porcelli, T., George, S. M., Zhou, Y., & Lian, J. (2016) Stabilizing an amorphous V 2 O 5/Carbon nanotube paper electrode with conformal TiO 2 coating by atomic layer deposition for Lithium ion batteries. Journal of Materials Chemistry A, 4(2), 537-544.

[80] Reiners, M., Xu, K., Aslam, N., Devi, A., Waser, R., & Hoffmann-Eifert, S. (2013) Growth and crystallization of TiO2 thin films by atomic layer deposition using a novel amido guanidinate titanium source and tetrakis-dimethylamido-titanium. Chemistry of Materials, 25(15), 2934-2943.

[81] Donders, M. E., Knoops, H. C. M., Kessels, W. M. M., & Notten, P. H. L. (2012) Co3O4 as anode material for thin film micro-batteries prepared by remote plasma atomic layer deposition. Journal of Power Sources, 203, 72-77.

[82] Baggetto, L., Niessen, R. A., Roozeboom, F., & Notten, P. H. (2008) High energy density all‐solid‐state batteries: a challenging concept towards 3D integration. Advanced Functional Materials, 18(7), 1057-1066.

[83] Golodnitsky, D., Nathan, M., Yufit, V., Strauss, E., Freedman, K., Burstein, L., ... & Peled, E. (2006) Progress in three-dimensional (3D) Li-ion microbatteries. Solid State Ionics, 177(26-32), 2811-2819.

[84] Nathan, M., Golodnitsky, D., Yufit, V., Strauss, E., Ripenbein, T., Shechtman, I., ... & Peled, E. (2005) Three-dimensional thin-film Li-ion microbatteries for autonomous MEMS. Journal of microelectromechanical systems, 14(5), 879-885.

[85] Ruzmetov, D., Oleshko, V. P., Haney, P. M., Lezec, H. J., Karki, K., Baloch, K. H., ... & Huang, J. (2011) Electrolyte stability determines scaling limits for solid-state 3D Li ion batteries. Nano letters, 12(1), 505-511.

[86] Lethien, C., Zegaoui, M., Roussel, P., Tilmant, P., Rolland, N., & Rolland, P. A. (2011) Micro-patterning of LiPON and lithium iron phosphate material deposited onto silicon nanopillars array for lithium ion solid state 3D micro-battery. Microelectronic engineering, 88(10), 3172-3177.

[87] Wang, C., Jia, G., Taherabadi, L. H., & Madou, M. J. (2005) A novel method for the fabrication of high-aspect ratio C-MEMS structures. Journal of microelectromechanical systems, 14(2), 348-358.

[88] Ribeiro, J. F., Sousa, R., Sousa, J. A., Pereira, B. M., Silva, M. F., Goncalves, L. M., ... & Correia, J. H. (2012) Rechargeable lithium film batteries–encapsulation and protection. Procedia Engineering, 47, 676-679.

[89] Koo, M., Park, K. I., Lee, S. H., Suh, M., Jeon, D. Y., Choi, J. W., ... & Lee, K. J. (2012) Bendable inorganic thin-film battery for fully flexible electronic systems. Nano letters, 12(9), 4810-4816.